Received: 23 May 2021 | Revised: 26 July 2021 | Accepted: 8 August 2021

DOI: 10.1002/app.51544

ARTICLE

Applied Polymer SCIENCE WILEY

Preparation and properties of colorless and transparent semi-alicyclic polyimide films with enhanced high-temperature dimensional stability via incorporation of alkyl-substituted benzanilide units

Xin-Xin Zhi | Gang-Lan Jiang | Yan Zhang | Yan-Jiang Jia | Lin Wu | Yuan-Cheng An | Jin-Gang Liu | Yan-gai Liu

Beijing Key Laboratory of Materials Utilization of Nonmetallic Minerals and Solid Wastes, National Laboratory of Mineral Materials, School of Materials Science and Technology, China University of Geosciences, Beijing, China

Correspondence
Jin-Gang Liu, Beijing Key Laboratory of Materials Utilization of Nonmetallic Minerals and Solid Wastes, National Laboratory of Mineral Materials, School of Materials Science and Technology, China University of Geosciences, Beijing 100083, China.
Email: liujg@cugb.edu.cn

Funding information
Shandong Key Research and Development Program, Grant/Award Number: 2019JZZY020235

Abstract

Two colorless and transparent polyimide (CPI) films with enhanced high-temperature dimensional stability and solution-processability were prepared from the methyl-substituted benzanilide containing organo-soluble polyimide (PI) resins. For this target, a new aromatic diamine, 2,3′-dimethyl-4,4′-diaminobenzanilide (MMDABA) was synthesized. The methyl substituents were expected to endow the derived PI resins good solubility and rigid-rod benzanilide units can efficiently reduce the coefficients of thermal expansion (CTE) of the derived CPI films. CPI-a and CPI-b were prepared by the one-step thermal polycondensation from MMDABA with hydrogenated pyromellitic dianhydride for CPI-a and hydrogenated 3,3′,4,4′-biphenyltetracarboxylic dianhydride for CPI-b, respectively. The derived PI resins were soluble in polar aprotic solvents. Colorless and transparent CPI-a and CPI-b films were prepared from the PI solutions and the subsequent 280°C curing. The CPI films showed good transparency in visible light and transmittances higher than 80% at 450 nm and yellowness index (b^*) below 2.0. More importantly, the derived CPI-a film showed the glass transition temperature (T_g) of 417.5°C and the CTE value of 46.9 × 10^{-6}/K in the range of 50–250°C. Apparently, incorporation of alkyl-substituted benzanilide units achieved good balance among solution-processability, high-temperature dimensional stability, and optical properties.

KEYWORDS

functionalization of polymers, polyimides, optical properties, thermal properties

1 | INTRODUCTION

Modern De-coloration of the standard wholly aromatic polyimide (PI) films, which are usually called "golden films," has been becoming one of the most active topics in the research and development of advanced PI films.[1,2] This is mainly due to the great potential applications of colorless and transparent PI (CPI) films in flexible electronic fabrications, such as flexible display, flexible photovoltaic, and so on.[3,4] There have mainly been two

Xin-Xin Zhi and Gang-Lan Jiang contributed equally to this study.

methodologies in the literature achieving the colorlessness of conventional wholly aromatic PI films up to now, including either introduction of nonconjugated molecular structures (aliphatic or alicyclic units, etc.) or incorporation of groups with high electronegativity (trifluoromethyl, etc.) in the PI molecular chains.[5] Both of these two methods are intended to prohibit or eliminate the formation of intra- and inter-molecular charge-transfer complexes (CTC) from the electron-donating diamine unit to the electron-withdrawing dianhydride moiety within the PI molecular chains.[6–10] Guided by this molecular design, two types of CPI films, including the semi-alicyclic and the fluoro-containing CPI films have been developed.[11,12] The semi-alicyclic CPI films, which are usually derived from the alicyclic dianhydrides and aromatic diamines, are characterized by the excellent solution-processability; excellent optical transparency (high optical transmittance, low yellow index, and low haze), good dielectric properties (low dielectric constant and dissipation factor), good thermal resistance, acceptable tensile properties, and relatively low cost.[13–15] Thus, they have been extensively investigated as functional components for advanced optoelectronic applications.[16–19] However, incorporation of alicyclic moieties might deteriorate some important properties for their practical applications, such as the dimensional stability at elevated temperatures, flame retardancy, and so on.[20–22] These disadvantages greatly hinder the wide applications of semi-alicyclic CPI films in advanced optical areas. Especially, the poor high-temperature dimensional stability of semi-alicyclic CPI films usually cause the mismatch of coefficients of linear thermal expansion (CTE) between the CPI films and the common low-CTE substrates, such as technical glasses (CTE $\approx$ 3–12 $\times$ 10^{-6}/K), quartz (CTE $\approx$ 3–8 $\times$ 10^{-6}/K), copper (CTE $\approx$ 17 $\times$ 10^{-6}/K), indium tin oxide (CTE $\approx$ 8 $\times$ 10^{-6}/K), and so on in optical devices.[23] The CTE mismatch of the components in microelectronic and optoelectronic devices is thought to be one of the most important factors deteriorating the reliability of the devices.[24] Thus, semi-alicyclic CPI films (CTE $\approx$ 60 $\times$ 10^{-6}/K) with reduced CTE values are highly desired for advanced optoelectronic applications.[25]

Generally, the high CTE features of the common semi-alicyclic CPI films, such as the one derived from hydrogenated pyromellitic dianhydride (HPMDA) and 4,4′-oxydianiline (ODA) (commercially available with the tradename of Neopulim® by Mitsubishi Gas Chemical, Japan), is mainly due to the easy movement of the alicyclic chain segments in the dianhydride units at elevated temperatures.[26] Thus, most of the modifications for developing semi-alicyclic PI films with intrinsically low CTE values have been focused on development of functional diamine monomers containing rigid units, such as amide, ester, benzimidazole, benzoxazole, and so on. Among the various rigid-rod groups, amide (—CONH—) or benzanilide (—Ph—CONH—Ph—) linkages show the best effects for reducing the CTE values of the CPI films while maintaining the intrinsic thermal, tensile, and optical properties.[27,28] Thus, various colorless and transparent PI films containing amide groups have been reported in the literature.[29,30] Hasegawa and coworkers reported the solution-processable CPI films based on an amide-containing diamine, AB-TFMB.[31] The rigid-rod amide (—CONH—) linkages in the diamine moiety endowed the CPI films CTE values as low as 7.3 $\times$ 10^{-6}/K in the temperature range of 100–200°C. Matsumoto et al. reported the semi-alicyclic CPI film derived from an alicyclic dianhydride, norbornane-2-spiro-α-cyclopentanone-α′-spiro-2″-norbornane-5,5″,6,6″-tetracarboxylic dianhydride (CpODA) and a benzanilide-containing diamine, 4,4′-diaminobenzanilide (DABA).[32] The derived CPI film showed a CTE value of 15.0 $\times$ 10^{-6}/K in the temperature range of 100–200°C. Although amide or benzanilide linkages could efficiently decrease the CTE values of CPI films, these rigid-rod groups often deteriorate the solubility of the CPI resins in organic solvents, thus sacrificing the solution-processability of the CPI films. The limited solubility of the amide or benzanilide-containing CPIs in organic solvents made it only possible to manufacture the CPI films by a two-step high-temperature thermal imidization process. The processing temperature as high as 300–350°C are definitely disadvantageous for the optical properties of the derived CPI films.

In the current work, as one of continuous efforts developing high-performance semi-alicyclic CPI films with enhanced high-temperature dimensional stability,[23] a series of CPI resins were first prepared from a newly developed alkyl-substituted benzanilide-containing aromatic diamine, 2,3′-dimethyl-4,4′-diaminobenzanilide (MMDABA) and alicyclic dianhydrides. In our previous work, in order to improve the organo-solubility of the benzanilide-containing CPI resins in organic solvents while maintaining the low-CTE feature of the derived CPI films, an aromatic diamine with single-methyl substituent, 2-methyl-4,4′-diaminobenzanilide (MeDABA) was designed and synthesized.[23] The derived CPI-R_a (HPMDA-MeDABA) and CPI-R_b (HBPDA-MeDABA) films exhibited good solubility in polar aprotic solvents, such as *N*-methyl-2-pyrrolidinone (NMP) and DMAc. The CPI-R_a (HPMDA-MeDABA) film derived from the CPI-R_a/DMAc solution exhibited high glass transition temperature (T_g) of 349°C and good dimensional stability at elevated temperatures with the CTE value as low as 33.4 $\times$ 10^{-6}/K in the temperature range of 50–250°C. However, in our following research developing CPI varnish for optoelectronic packaging, the CPI-R_a solution showed unsatisfied storage stability at high solid contents ($\geq$35 wt%), which might be due to the inadequate solubility

of the CPI-R_a resin in the solvent of DMAc. Thus, a new aromatic diamine, MMDABA was currently designed and synthesized, in which two methyl substituents were introduced in order to achieve a higher solubility of the derived semi-alicyclic CPI resins. Meanwhile, the CTE values of the derived CPI films were expected to be maintained at a relatively low level. The Effects of the methyl substituents, benzanilide linkages, and alicyclic units on the solution-processability, thermal, and optical properties of the CPIs were investigated in detail.

2 | EXPERIMENTAL

2.1 | Materials

Polymerization-grade (purity ≥99.5%) hydrogenated pyromellitic anhydride (HPMDA) and hydrogenated 3,3′,4,4′-biphenyltetracarboxylic dianhydride (HBPDA) were purchased from Weihai Newera Kesense New Materials Co. Ltd. (Shandong, China) and dried at 180°C in vacuo for 24 h prior to use. 2-methyl-4-nitrobenzoyl chloride (MNC) and 2-methyl-4-nitroaniline (MNA) were purchased from Tokyo Chem. Ind. Co, Ltd. (TCI, Tokyo, Japan) and used as received. Electronic grade γ-butyrolactone (GBL) was purchased from Greenda Chem. Co. Ltd., China (Hangzhou, Zhejiang, China) and used as received. NMP was purchased from InnoChem Sci. Technol. Co. Ltd. (Beijing, China) and was vacuum distilled over phosphorus pentoxide (P_2O_5) prior to use. *N,N*-dimethylacetamide (DMAc) was purchased from Sinopharm Chem. Reagent Co. Ltd., and distilled over CaH_2 prior to use. The other commercially available reagents and materials were all purchased and used as received.

2.2 | Measurements

Inherent viscosity was measured using an Ubbelohde viscometer with a 0.5 g/dl NMP solution at 25°C. Attenuated total reflectance Fourier transform infrared (ATR-FTIR) spectrum was obtained on a Bruker Tensor-27 FT-IR spectrometer. ^{1}H-NMR was performed on an AV 400 spectrometer operating at 300 MHz using DMSO-d_6 as the solvent and tetramethylsilane as the reference. Ultraviolet–visible (UV–Vis) spectra of the PI films were recorded on a Hitachi U-3210 spectrophotometer at room temperature. Prior to test, PI samples were dried at 100°C for 1 h to remove the absorbed moisture. The number average molecular weight (M_n) and weight average molecular weight (M_w) of the PI resins were measured using a gel permeation chromatography system developed by Shimadzu Co. Ltd., Japan with a LC-20 AD dual-plunger parallel-flow pumps (D1-LC), a SIL-20A is a total-volume injection-type autosampler, a CTO-20A column oven, and a RID-20A detector. HPLC grade NMP was used as the mobile phase at a flow rate of 1.0 ml/min. Polystyrene (Shodex, Type: SM-105, Showa Denko Co. Ltd., Japan) was used as the standard. Wide-angle X-ray diffraction (XRD) was conducted on a Rigaku D/max-2500 X-ray diffractometer with Cu-Kα1 radiation, operated at 40 kV and 200 mA. UV–Vis spectra were recorded on a Hitachi U-3210 spectrophotometer at room temperature. Prior to test, PI films were dried at 100°C for 1 h to remove the absorbed moisture. Yellow index and haze values of the PI films were measured using an X-rite color i7 spectrophotometer with PI film samples at a thickness of 25 μm. The color parameters were calculated according to a Commission Internationale de l'Eclairage (CIE) Lab equation. L^* is the lightness, where 100 means white and 0 implies black. A positive a^* means a red color, and a negative one indicates a green color. A positive b^* means a yellow color, and a negative one indicates a blue color.

Thermogravimetric analysis (TGA) was performed on a TA-Q50 thermal analysis system at a heating rate of 20°C/min in nitrogen. Dynamic mechanical analysis (DMA) was recorded on a TA-Q800 thermal analysis system at a heating rate of 5°C/min and a frequency of 1 Hz in nitrogen. Thermo-mechanical analysis (TMA) was recorded on a TA-Q 400 thermal analysis system in nitrogen at a heating rate of 10°C/min.

Solubility was determined as follows: 1.0 g of the tested PI resin was mixed with 9.0 g of the solvent at room temperature (10 wt% solid content), which was then mechanically stirred in nitrogen for 24 h. The solubility was determined visually as three grades: completely soluble (++), partially soluble (+), and insoluble (−). The complete solubility is defined as a homogenous and clean solution is obtained, in which no phase separation, precipitation or gel formation is detected.

2.3 | Synthesis of 2,3′-dimethyl-4,4′-diaminobenzanilide

MMDABA was synthesized in our laboratory with MNC and MNA as the starting materials according to the similar procedure reported in the literature and purified by recrystallization from absolute ethanol.[23] MMDABA was obtained as colorless needles with the purity of 99.5% according to the gas chromatography analysis. Yield: 57%. Melting point: 185.4°C (differential scanning calorimetry (DSC) peak temperature). FT-IR (KBr, cm^{-1}): 3460, 3341, 3249, 3213, 2967, 2920, 1628, 1570, 1485, 1288, 1153, 833, and 768. ^{1}H-NMR (300 MHz, DMSO-d_6, ppm): 9.09 (s, 1H), 7.59–7.53 (m, 2H), 6.86–6.82 (m, 1H),

6.61–6.57 (m, 1H), 6.42–6.35 (m, 2H), 5.39 (s, 2H), 4.90 (s, 2H), and 2.10–2.03 (m, 6H). Elemental analysis: $C_{12}H_{13}N_3$: Cald. C, 72.33%, H, 6.58%, N, 21.09%; Found: C, 72.17%, H, 6.63%, N, 21.03%.

2.4 | Preparation of PI resins and films

The CPI resins were prepared from MMDABA and HPMDA or HBPDA via a one-step high-temperature polycondensation procedure. CPI-a (HPMDA-MMDABA) resin was taken as an example to show the detailed synthesis procedure. Into a 500 ml three-necked, round-bottomed flask equipped with a mechanical stirrer, a heating equipment, a Dean-Stark trap and a nitrogen inlet was charged with MMDABA (25.5310 g, 100 mmol) and GBL (100.0 g) at room temperature (25°C). Then, to the clear diamine solution, HPMDA (22.4170 g, 100 mmol) was added in one batch and an additional volume of GBL (43.8 g) was added to wash the residual dianhydride, and at the same time to adjust the solid content of the reaction system to be 25 wt%. After stirring in nitrogen for 1 h, the toluene dehydrating agent (200 ml) and the triethylamine catalyst (1.0 g) was added. The reaction mixture was then heated to 180°C to facilitate the imidization reaction, during which the water by-products were distilled out of the reaction system via the toluene azeotrope at 130–140°C for 6 h. The high temperature imidization reaction continued at 180°C for 3 h, and then cooled to room temperature. The obtained pale-brown and viscous solution was slowly dripped into an excess of aqueous ethanol solution (concentration: 80 wt %). The precipitated fibrous PI-a resin was collected and dried at 80°C under vacuum for 24 h. CPI-a was obtained as white fibrous resin.

Yield: 42.57 g (96.0%). ^{1}H-NMR (DMSO-d_6, ppm): 10.11 (s, 1H), 8.02–7.96 (m, 1H), 7.52–7.45 (m, 1H), 7.30–7.26 (m, 1H), 7.24–7.16 (m, 2H), 3.25 (m, 4H), 2.34–2.30 (m, 6H), 2.23–2.17 (m, 2H), and 2.13–2.00 (m, 2H).

The fully dried PI-a resin was dissolved into DMAc at a solid content of 20 wt% to obtain the PI solution. The solution was stirred at room temperature overnight and then filtered through a 0.25 μm Teflon syringe filter to remove any impurities. The purified PI-a varnish was used for the film preparation. Colorless and transparent PI-a film was obtained by thermally baking the solution in a nitrogen flow according to the following heating procedure: 80°C/2 h, 150°C/1 h, 200°C/1 h, 250°C/1 h, and 280°C/1 h.

CPI-b resin and film were prepared according to the similar procedures as mentioned above except HBPDA (30.6310 g, 100 mmol) was used instead of HPMDA (22.4170 g, 100 mmol). CPI-b resin. Yield: 50.46 g (96.0%). ^{1}H-NMR (DMSO-d_6, ppm): 10.05 (s, 1H), 7.97–7.89 (m, 1H), 7.48–7.46 (m, 1H), 7.40–7.35 (m, 1H), 7.22–7.14 (m, 2H), 3.37–3.23 (m, 2H), 3.09–3.00 (m, 2H), 2.28 (m, 3H), 2.19 (m, 3H), 2.17–2.05 (m, 4H), 1.65 (m, 4H), 1.33–1.21 (m, 4H), and 1.03–1.01 (m, 2H).

Two CPI references containing single-methyl substituent in the molecular structure, including CPI-R_a and CPI-R_b were prepared by the one-step high-temperature polycondensation procedure from 2-methyl-4,4′-diaminobenzanilide (MeDABA) and HPMDA for CPI-R_a and HBPDA for CPI-R_b, respectively.[23]

3 | RESULTS AND DISCUSSION

3.1 | Monomer synthesis

MMDABA was synthesized via a two-step procedure with the total yield of 57%. Firstly, 2,3′-dimethyl-4,4′-dinitrobenzanilide (MMDNBA) was synthesized from 2-methyl-4-nitrobenzoyl chloride (MNC) and 2-methyl-4-nitroaniline (MNA). Secondly, the MMDNBA was reduced by hydrazine hydrate ($NH_2NH_2{\cdot}H_2O$) in ethanol under the catalysis of Pd/C. After recrystallization in absolute ethanol, MMDABA was obtained as colorless crystals.

Figure 1 shows the ATR-FTIR spectrum of MMDABA, in which the characteristic absorptions of primary amine (—NH_2) at the wavenumber of 3460 and 3341 cm^{-1}, the absorption of secondary amine (—CONH—) at 3249 cm^{-1}, the absorptions of saturated C—H bonds (—CH_3) at 2967 cm^{-1} and 2920 cm^{-1}, the absorption of carbonyl (—CONH—) at 1628 cm^{-1}, and the absorptions of C=C bonds in benzene at 1570 and 1485 cm^{-1} could be clearly

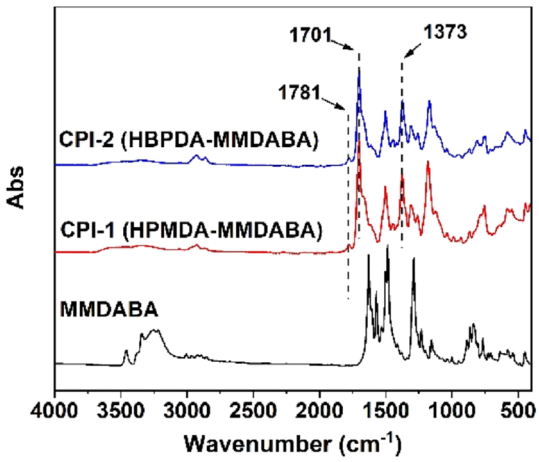

FIGURE 1 ATR-FTIR spectra of MMDABA and the derived PI films. ATR-FTIR, attenuated total reflectance Fourier transform infrared [Color figure can be viewed at wileyonlinelibrary.com]

observed. The chemical structure of MMDABA can be further confirmed by the ^{1}H-NMR measurement, as shown in Figure 2. The spectrum reveals 11 kinds of proton absorptions, which are in good consistent with the expected molecular structure of MMDABA. The amide proton (—CONH—) showed the absorption at the farthest downfield (chemical shift: ~9.0 ppm) in the spectrum due to the existence of strong electron-withdrawing carbonyl group. The protons at the *ortho*-substituted positions to the carbonyl group in amide (H_1 and H_3) showed the absorptions at the second farthest downfield (chemical shift: ~7.5 ppm) in the spectrum. The protons in the two amino groups (—NH_2, ① and ②) and in the two methyl groups (—CH_3, ③ and ④) exhibited individual absorptions, respectively, due to the different chemical circumstances of the protons. This is also in good agreement with the structural characteristics of the MMDABA diamine. The elemental analysis results also supported the successful preparation of the novel alkyl-substituted benzanilide diamine.

3.2 | PI synthesis and film preparation

Polymerization-grade MMDABA was polymerized with two alicyclic dianhydrides, HPMDA and HBPDA, respectively, to afford two PI resins, CPI-a (HPMDA-MMDABA) and CPI-b (HBPDA-MMDABA). Due to the good solubility of the obtained PI resins in the polymerization solvent (GBL), the one-step polycondensation procedure was successfully carried out, as shown in Figure 3. During the dehydration procedure via toluene azeotrope and the following high-temperature polymerization, the reaction system consistently maintained homogeneous, and no gelling or precipitating occurred. According to the similar procedure, two referenced PI resins, including CPI-R_a (HPMDA-MeDABA) and CPI-R_b (HBPDA-MeDABA) were also prepared, whose chemical structures are shown in Figure 4. It could be clearly observed from Figures 3 and 4 that the PIs derived from MMDABA and MeDABA diamines possessed asymmetrical molecular structures due to the asymmetric nature of the starting diamines. This structural feature could usually bring some advantages and disadvantages to the polymers. The advantages usually lie in the improved solubility of the derived PI resins and enhanced optical transparency of the final PI films due to the reduced molecular chains packing density.[33] The disadvantages are usually related with the different reactivity of the active amino groups. For example, for MMDABA, the —NH_2 group adjacent to —CH_3 (① in Figure 2) usually had higher reactivity than another —NH_2 group (② in Figure 2) for the reaction generating amide acid due to the higher electron density afforded by the electron-donating methyl group.[34] This might cause the head-to-head and head-to-tail sequences in the PI structures.

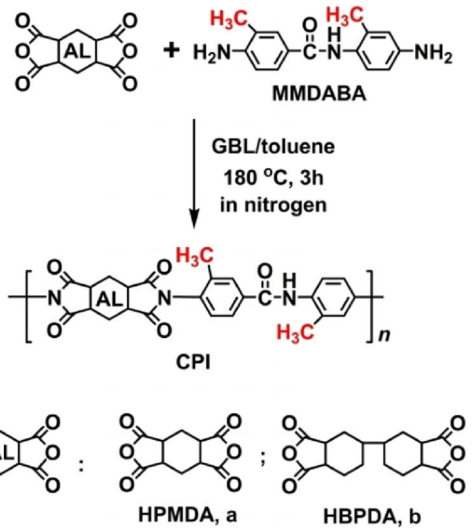

FIGURE 3 Preparation of MMDABA-PI resins [Color figure can be viewed at wileyonlinelibrary.com]

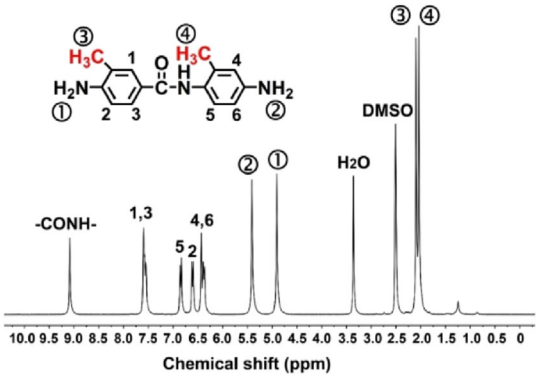

FIGURE 2 ^{1}H-NMR spectrum of MMDABA (in DMSO-d_6) [Color figure can be viewed at wileyonlinelibrary.com]

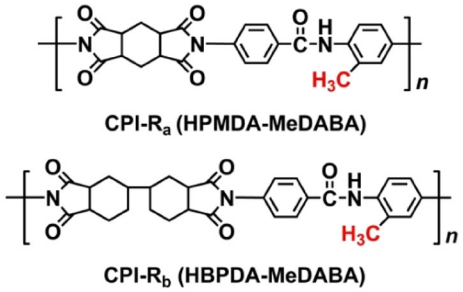

FIGURE 4 Chemical structures of the CPI reference films [Color figure can be viewed at wileyonlinelibrary.com]

Nevertheless, this disadvantage had little effects on the properties of the derived PI films.

The CPI resins were obtained as white and silky solids with the intrinsic viscosities of 0.72 dl/g for CPI-a and 0.87 dl/g for CPI-b, respectively, as shown in Table 1. The CPI resins showed the number average molecular weights (M_n) in the range of 2.44×10^4–4.81×10^4 g/mol and the PDI values of 1.73–1.77. The moderate to high intrinsic viscosities and M_n values of the current CPI resins indicate the good reactivity of the MMDABA diamine when polymerizing with the alicyclic dianhydrides. The relatively low PDI values indicated that few side reactions occurred during the high-temperature polymerization. The high-molecular-weight feature of the current CPI resins is quite beneficial for obtaining the CPI films with high flexibility and toughness. The CPI resins showed good solubility in polar aprotic solvents, including NMP, DMAc, and GBL. CPI-b was soluble even in chloroform (Table 1). The good solubility of the CPI resins in organic solvents makes it possible to fabricate the CPI films via solution-processing procedure in the imide forms. Thus, much lower processing temperature could be adopted for the CPI film fabrication, which is only to physically evaporate the solvent instead of chemically inducing the imidization of the poly(amic acid) precursors via dehydration. The lower processing temperature could usually guarantee the optical transparency of the derived CPI films to the maximum extent.

Although the current CPI resins showed comparable solubility with that of the references CPI-R_a and CPI-R_b resins,[23] the CPI-a and CPI-b solution showed much better storage stability at the high solid contents of 35 wt%. In our storage evaluation, both of the CPI-a and CPI-b varnish obtained by dissolving the CPI resins in the solvent mixture of DMAc and butyl cellulose (BC) (DMAc/BC = 80:20, weight ratio) at the solid content of 35 wt% showed good stability more than 1 year. However, apparent increase of the solution viscosities or gelling occurred for the analogous CPI-R_a varnish at the same solid content within 6 months. The main reason of this phenomenon might be due to the relatively poor solubility of CPI-R_a resin in the solvents. Undoubtedly, two methyl substituents in the repeating units of the CPI resins apparently increased the solubility of the current polymers in the solvents.

The good solubility of the current CPI resins in polar solvents makes it possible to confirm the chemical structure of the polymers. Figure 5 shows the ^{1}H-NMR spectra of the CPI resins. The two polymers exhibited similar absorptions in the downfield areas in the spectra caused by the aromatic protons in the MMDABA moiety. It is similar with the spectrum of MMDABA diamine (Figure 2), the absorptions of the protons in the amide (—CONH—) groups were observed at the farthest downfield in the spectra for both of the polymers. The protons in the phenyl rings (H_1–H_6) induced absorptions at the second farthest downfield in the range of 7.0–8.0 ppm in the spectra. The protons in the alicyclic dianhydride units and in methyl substituents showed absorptions at the upfield areas in the spectra. Due to the different chemical environments of the proton pairs in the cyclohexane rings in the dianhydrides, including $H_{b,b'}$ for HPMDA, and $H_{b,b'}$, $H_{d,d'}$, and $H_{e,e'}$ for HBPDA, they revealed different signals in the spectra. These structural characteristics revealed by the spectra confirmed the successful preparation of the resins.

Flexible and tough CPI films were also successfully obtained by casting the CPI solutions onto clean glass plates, followed by thermally curing at elevated temperatures from 80 to 280°C. A step-heating curing procedure was used for the preparation of the films in order to prevent the surface and internal defects of the films caused by the fast heating. The freestanding CPI films showed colorless and transparent appearance with smooth surface. The chemical structures of the films were confirmed by the ATR-FTIR measurements, as shown in Figure 1. In the spectra, the characteristic absorptions of amino in MMDABA (3460 and 3341 cm^{-1}) disappeared in the spectra of PI films. Instead, the characteristic absorptions of imide rings, including those at 1781 and 1703 cm^{-1}, assigned to the asymmetric and symmetric carbonyl stretching vibrations, respectively, and the ones at 1373 cm^{-1} due to the C—N stretching vibration could be

TABLE 1 Inherent viscosities, molecular weights, and solubility of the MMDABA-PI resins

		Molecular weight[b]			Solubility[c]				
PI	$[\eta]_{inh}$[a] (dl/g)	M_n ($\times 10^4$ g/Mol)	M_w ($\times 10^4$g/Mol)	PDI	NMP	DMAc	GBL	CPA	$CHCl_3$
CPI-a	0.87	4.81	8.34	1.73	++	++	++	−	+
CPI-b	0.72	2.44	4.32	1.77	++	++	++	+−	++

[a]Inherent viscosities measured with a 0.5 g/dl PI solution in NMP at 25°C.

[b]M_n, number average molecular weight; M_w, weight average molecular weight; PDI, polydispersity index, PDI = M_w/M_n.

[c]++, Soluble; +, partially soluble; −, insoluble. GBL, γ-butyrolactone; CPA, cyclopentanone; THF, tetrahydrofuran.

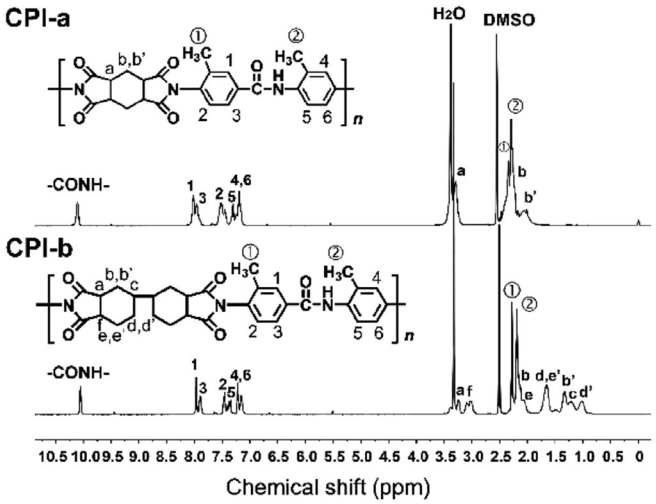

FIGURE 5 ^{1}H-NMR spectra of MMDABA-PI resins

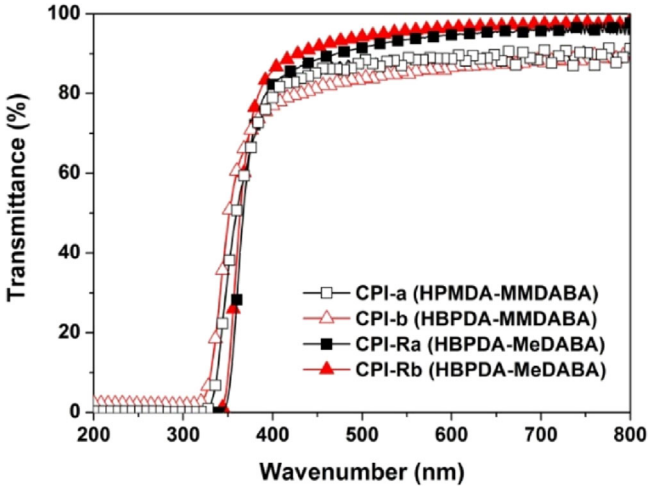

FIGURE 6 UV–vis spectra of CPI films [Color figure can be viewed at wileyonlinelibrary.com]

obviously observed for the PI films. In addition, the characteristic absorptions of C═C bonds in phenyl ring and the saturated C—H bonds in methyl and cyclohexane rings were also detected in the spectra of the PI films.

3.3 | Optical properties

It has been well-established that the optical properties of the PI films are usually predominantly affected by the dianhydride moiety. The semi-alicyclic CPI films usually possess excellent optical properties due to the highly prohibited CT interactions in the PI molecular chains. From this point of view, the optical transparency of the semi-alicyclic CPI films should be better than that of the fluoro-containing counterpart. After all, in the molecular chains of fluoro-containing CPIs, the CT interactions still exist although they are often inhibited by the highly electronegative fluoro-containing groups. Thus, it can be predicted that the current benzanilide-containing semi-alicyclic CPI films should have acceptable optical transparency and color parameters even if the existence of photo sensitive —CONH— bonds in the PIs. The effects of the dianhydride and diamine structures of the PI films on the optical properties, including optical transmittance, and CIE Lab parameters of the CPI films were investigated.

First, Figure 6 shows the UV–Vis spectra of the PI films at a thickness of 25 μm. The optical data, including ultraviolet cutoff wavelengths (λ_{cut}), and the transmittances at the wavelength of 450 nm (T_{450}) of the PI and referenced PI films are summarized in Table 2. It can be deduced from the data that the semi-alicyclic benzanilide-containing CPI films, either the MeDABA-PIs or the MMDABA-PIs, showed good optical transparency in the ultraviolet-visible light region with the λ_{cut} values in the range of 315–341 nm and transmittances higher than 80% at 450 nm. The good optical transparency of the semi-alicyclic CPI films is mainly attributed to the nonconjugated alicyclic dianhydride structure. Comparatively, the single-methyl-substituted referenced CPI films showed a little better optical transparency than that of the double-methyl-substituted MMDABA-PI films when the wavelength was higher than 400 nm. For example, CPI-R_a showed a T_{450} value of 88.6%, which is 2.2% higher than that of PI-a. The relatively inferior optical transparency of the MMDABA-PI films to MeDABA-PI films at the higher wavelength region might be due to the higher Fresnel reflection at the MMDABA-PI film surfaces,[35] which will be investigated in detail in our future work.

Figure 7 shows the CIE Lab optical parameters of the MMDABA-PI films. The CPI films showed the yellow indices (b^*) of 1.82 for CPI-a and 1.78 for CPI-b, which are comparable to the PI reference films ($b^* = 2.18$ for CPI-R_a and $b^* = 1.92$ for CPI-R_b). The low yellowness of the current CPI films is mainly associated with the absence or inhibition of intra- and/or inter-molecular CT interactions between the electron-donor (diamine) and electron-acceptor (dianhydride) moieties in the PI molecular chains. Introduction of nonconjugated alicyclic structure in the PI skeletons efficiently reduced the formation of CTC, thus reducing the coloration of PI films. In addition, the CPI and referenced CPI films exhibited close haze values. Generally, the generation of haze of polymeric optical films is mainly due to the scattering of light by the film, either due to the surface effects or internal structure effects in the polymers.[36] The micro-sized irregularities in the refractive index arising primarily from the crystalline structure of the polymers have been thought to be the main reason for the high haze values of

TABLE 2 Optical and thermal properties of the CPI films

	Optical properties[a]				Thermal properties[b]				
PI	λ_{cut} (nm)	T_{450} (%)	b^*	Haze (%)	$T_{5\%}$ (°C)	R_{w700} (%)	$T_{g,\ DSC}$ (°C)	$T_{g,\ DMA}$ (°C)	CTE ($\times 10^{-6}$/K)
CPI-a	326	86.4	1.82	2.79	459.4	42.3	-[c]	417.5	46.9
CPI-b	315	81.5	1.78	1.28	459.3	31.1	294.9	326.3	62.9[d]
CPI-R_a	341	88.6	2.18	2.15	438.1	44.6	349.1	347.3	33.4
CPI-R_b	338	91.7	1.92	1.07	466.3	24.4	265.3	278.0	55.3

[a]λ_{cut}, cutoff wavelength; T_{450}, transmittance at the wavelength of 450 nm; b^*, yellow index.
[b]$T_{5\%}$, temperatures at 5% weight loss; R_{w700}, residual weight ratio at 700°C in nitrogen; $T_{g,DSC}$, glass transition temperature detected by DSC measurements; $T_{g,DMA}$, glass transition temperature detected by DMA measurements; CTE, linear coefficient of thermal expansion in the range of 50–250°C.
[c]Not observed in the temperature range of 50–400°C.
[d]CTE value in the range of 50–200°C.

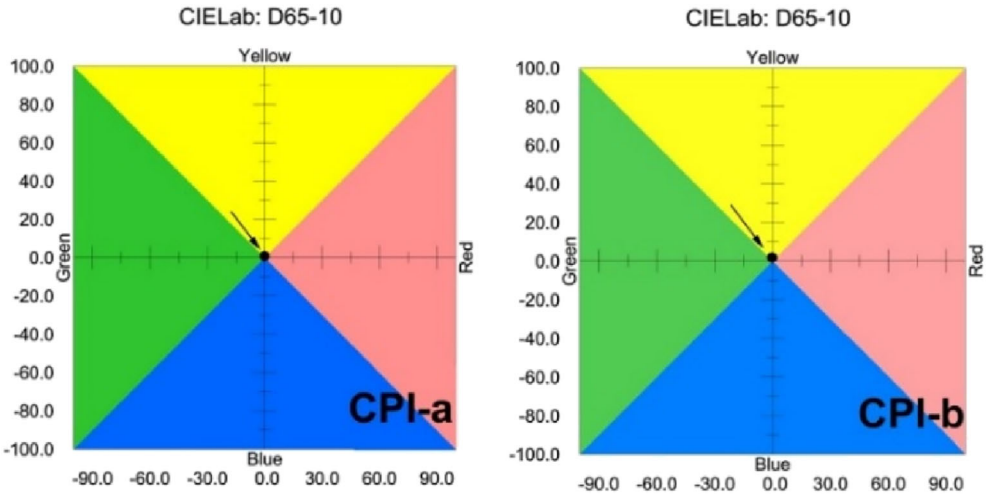

FIGURE 7 CIE lab parameters of MMDABA-PI films [Color figure can be viewed at wileyonlinelibrary.com]

polymer films.[37] As for the current semi-alicyclic PI films, they showed quite low haze values, indicating the low inhomogeneity in the films. This is mainly attributed to the amorphous nature of the polymer films, evidenced by the XRD measurements shown in Figure 8. Although amide (—CONH—) bonds are usually easy to induce the crystallization of the molecular chains, leading to the increase of the haze values of the films, the crystalline degree of the current semi-alicyclic PIs was efficiently confined to a low level due to the loose molecular packing and less-interacted cyclohexane rings in the dianhydride unit.

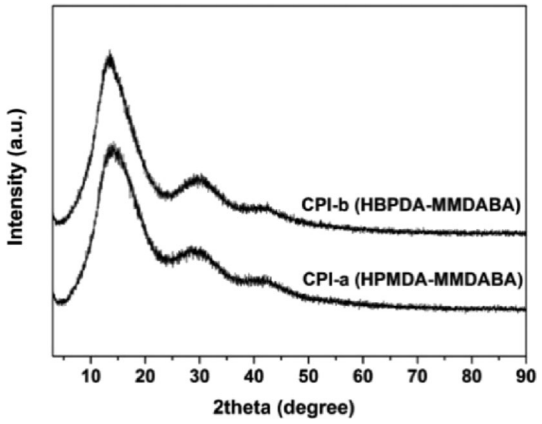

FIGURE 8 XRD patterns of MMDABA-PI films. XRD, X-ray diffraction

3.4 | Thermal properties

Good solution-processability in the imide form, good optical transparency in the visible light region, and good thermal and dimensional stability are usually highly desired for the applications of CPI films in high-tech areas. However, these property requirements are usually inter-constraint in most CPI materials. The methodologies improving the solution-processability and optical transparency of the CPIs, such as incorporation of non-conjugated alicyclic units and flexible linkages, usually deteriorate the thermal and dimensional stability of the CPI films. Introduction of rigid-rod linkages in the dianhydride and diamine moieties while regulating

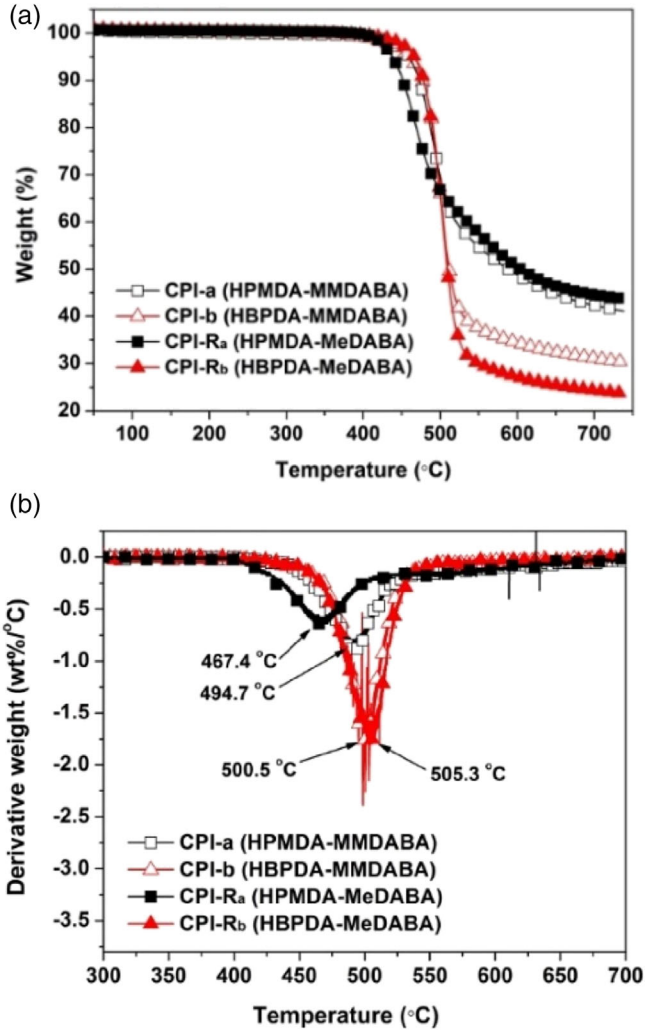

FIGURE 9 Thermal decomposition plots of MMDABA-PI films in nitrogen. (a) TGA; (b) DTG. TGA, thermogravimetric analysis [Color figure can be viewed at wileyonlinelibrary.com]

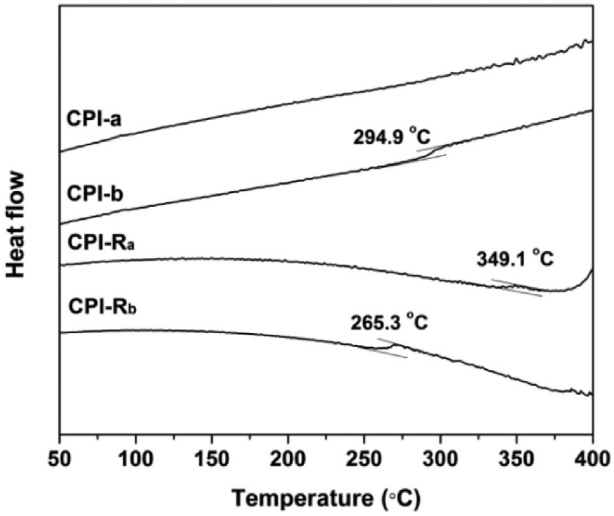

FIGURE 10 DSC plots of CPI films

and controlling the solubility of the CPIs so as to achieve a balance among the property requirements has been proven to be one of the most effective procedures for developing high-performance CPI films. In the current work, the thermal properties, including thermal decomposition, glass transition, dynamical mechanical, and thermal mechanical behaviors of the CPI films were investigated and tabulated in Table 2. Both of the CPI films and the referenced CPI films showed good thermal stability with the 5% weight loss temperatures ($T_{5\%}$) in the range of 438.1–466.3°C and residual weight ratios at 700°C of 24.4%–44.6%, as observed from the TGA plots of the CPI films (Figure 9a). All the CPI films showed good thermal stability up to 400°C, after which the polymers began to decompose and showed the maximum decomposition temperatures higher than 460°C, evidenced by the DTG plots (Figure 9b).

The glass transition temperatures (T_g) of the CPI films were measured by both DSC and DMA methods, as illustrated by Figure 10 (DSC) and Figure 11 (DMA), respectively. As we know, different polymers usually showed different response or sensitivity to varied T_g measurements, such as DSC, DMA, and TMA. Thus, different modes of T_g measurements usually reveal quite different T_g values for the same polymer. In the current work, the T_g values of CPI films are influenced by both of the dianhydride and the diamine moieties. For example, for the same dianhydride HPMDA, the CPI film derived from MMDABA (CPI-a) showed higher T_g value than MeDABA (CPI-R_a). For the same diamine MMDABA, the CPI film derived from HPMDA (CPI-a) showed higher T_g value than that of HBPDA (CPI-b). Although CPI-a did not show clear glass transition in the DSC measurement from room temperature to 400°C (the upper limitation of the machine), it showed the clear T_g value of 417.5°C in the DMA measurement recorded as the peak of tan delta plot. This high T_g for CPI-a is mainly attributed to the rigid-rod benzanilide unit and the pendant methyl substituents. Especially, the *ortho*-substituted methyl to the amino group would prohibit the movement of the CPI-a molecular chain along the main chain, thus greatly increasing the T_g value of the polymer.[38] This high-T_g feature is quite beneficial for the application of CPI-a film in flexible electronic fabrications, in which high temperature procedures over 400°C are usually desired.[39] Similarly, CPI-b also exhibited high T_g value of 294.9°C for DSC and 326.3°C for DMA measurements. Comparatively, the analogous CPI-R_b film showed inferior T_g value of 265.3°C for DSC and 278.0°C for DMA measurements. The reduced T_g value of CPI-R_b film is undoubtedly due to the absence of *ortho*-substituted methyl in the molecular structure. In addition, it can be observed from Figure 11 that the CPI-a film showed an initial storage modulus of 3.2 GPa at

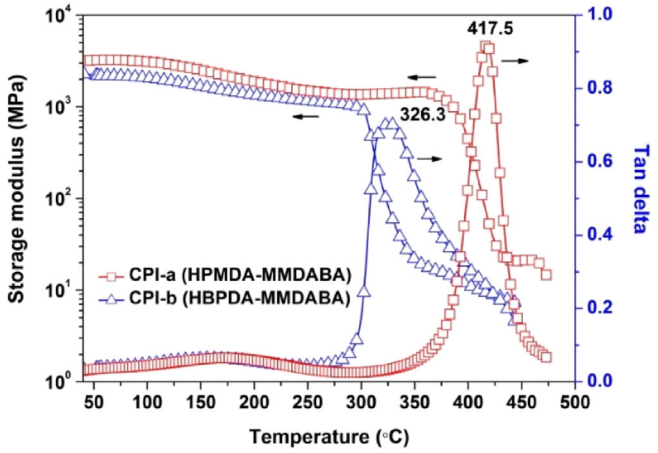

FIGURE 11 DMA curves of MMDABA-PI films [Color figure can be viewed at wileyonlinelibrary.com]

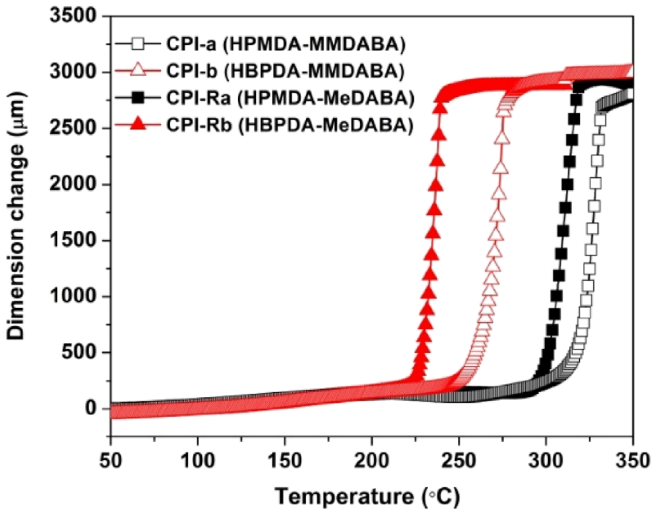

FIGURE 12 TMA curves of MMDABA-PI films. TMA, thermo-mechanical analysis [Color figure can be viewed at wileyonlinelibrary.com]

room temperature, which was 1.4 GPa at the temperature of 350°C. Thus, nearly 44% of the initial storage modulus was maintained at 350°C, indicating good thermal stability of the film.

At last, the dimensional stability of the CPI films at elevated temperature was evaluated by TMA measurements, as shown in Figure 12. The recorded coefficients of linear thermal expansion (CTE) values of the films in the range of 50–250°C are listed in Table 2. As expected, the CPI films derived from flexible HBPDA dianhydride, including CPI-b and CPI-R_b showed high CTE values over 55.0 × 10^{-6}/K, indicating poor dimensional stability of the polymers even rigid-rod benzanilide-containing diamines were used. The CPI films derived from more rigid HPMDA dianhydride showed apparently reduced CTE values. CPI-a exhibited a CTE value of 46.9 × 10^{-6}/K from 50 to 250°C, which is higher than that of CPI-R_a (CTE: 33.4 × 10^{-6}/K). Thus, the incorporation of another methyl in the repeating unit of the CPI polymer slightly deteriorated the high-temperature dimensional stability of the film. Nevertheless, the CPI-a film showed apparently reduced CTE value than that of the commercially available CPI film based on HPMDA, such as Neopulim® L-3430 (CTE = 58.0 × 10^{-6}/K).[26] The low-CTE feature of CPI-a film is quite beneficial for the further decreasing the CTE value of the film via incorporation of inorganic nano-fillers. Small quantity of nano-fillers might be needed to achieve the lower CTE of the composite films. On the other hand, the current CTE values of the CPI-a film was obtained by the laboratory-made sample without any orientation. In the industrial production, the biaxially stretching treatment to the CPI-a film might induce the efficient orientation of the molecular chains, which is thought to be quite helpful for reducing the CTE and enhancing the dimensional stability of the film at elevated temperatures.

4 | CONCLUSIONS

This work attempts to develop high-performance CPI films with excellent high-temperature dimensional stability (low CTE), good solution-processability, and improved optical properties. A series of measurements showed that the introduction of benzanilide linkage and alkyl substituents in the diamine moiety and the introduction of alicyclic units in the dianhydride moiety is the effective pathway to achieve the target above. For the PI films containing benzanilide units in the structure, the substitute effects played important roles affecting the properties of the derived polymers. The PIs derived from DABA usually exhibited poor solution-processability due to the rigid molecular skeletons and strong inter- and intramolecular actions. Incorporation with single —CH_3 group into the DABA (MeDABA) could endow the PIs good solubility in organic solvents although the CTE values might increase simultaneously. However, the storage stability of the MeDABA-PI solutions was not satisfying. For the PIs derived from double —CH_3 groups (MMDABA), the developed CPI-a (HPMDA-MMDABA) resin showed good solubility in the polar aprotic solvents. The CPI-a/DMAc/BC varnish system with the solid content of 35 wt % showed good stability more than 1 year. The CPI-a film cast from the CPI-a/DMAc solution showed good combined properties with the $T_{5\%}$ value of 459.4°C, the T_g value of 417.5°C by DMA, the T_{450} value of 86.4%, and the CTE value of 46.9 × 10^{-6}/K in the temperature range of 50–250°C. Such good comprehensive properties make

the current CPI-a film a good candidate as high-performance optical components for advanced optical applications.

ACKNOWLEDGMENTS

Financial support from the Shandong Key Research and Development Program (No. 2019JZZY020235) is gratefully acknowledged.

ORCID

Jin-Gang Liu https://orcid.org/0000-0001-6629-1646

REFERENCES

[1] P. K. Tapaswi, C. S. Ha, *Macromol. Chem. Phys.* **2019**, *220*, 1800313.
[2] M. C. Choi, Y. Kim, C. S. Ha, *Prog. Polym. Sci.* **2008**, *33*, 581.
[3] H. Min, B. Kang, Y. S. Shin, B. Kim, S. W. Lee, J. H. Cho, *ACS Appl. Mater. Interfaces* **2020**, *12*, 18739.
[4] J. H. Chang, *Rev. Adv. Mater. Sci.* **2020**, *59*, 1.
[5] C. Yi, W. Li, S. Shi, K. He, P. Ma, M. Chen, C. Yang, *Sol. Energy* **2020**, *195*, 340.
[6] H. J. Ni, J. G. Liu, Z. H. Wang, S. Y. Yang, *J. Ind. Eng. Chem.* **2015**, *28*, 16.
[7] Y. Zhang, L. Qu, J. Liu, X. Wu, Y. Zhang, R. Zhang, H. Qi, X. Zhang, *J. Coat Technol. Res.* **2019**, *16*, 511.
[8] H. H. Kim, H. J. Kim, B. J. Choi, Y. S. Lee, S. Y. Park, L. S. Park, *Mol. Cryst. Liq. Cryst.* **2013**, *584*, 153.
[9] S. D. Kim, S. Lee, J. Heo, S. Y. Kim, I. S. Chung, *Polymer* **2013**, *54*, 5648.
[10] A. I. Wozniak, A. S. Yegorov, V. S. Ivanov, S. M. Igumnov, K. V. Tcarkova, *J. Fluorine Chem.* **2015**, *180*, 45.
[11] F. Li, J. Liu, X. Liu, Y. Wang, X. Gao, X. Meng, G. Tu, *Polymer* **2018**, *10*, 546.
[12] Y. Yang, J. H. Park, Y. Jung, S. G. Lee, S. K. Park, S. Kwon, *J. Appl. Polym. Sci.* **2017**, *134*, 44375.
[13] T. Matsumoto, D. Mikami, T. Hashimoto, M. Kaise, R. Takahashi, S. Kawabata, *J. Phys.: Conf. Ser.* **2009**, *187*, 012005.
[14] K. Fukukawa, M. Okazaki, Y. Sakata, T. Urakami, W. Yamashita, S. Tamai, *Polymer* **2013**, *54*, 1053.
[15] D. J. Liaw, K. L. Wang, Y. C. Huang, K. R. Lee, J. Y. Lai, C. S. Ha, *Prog. Polym. Sci.* **2012**, *37*, 907.
[16] Y. Zhuang, J. G. Seong, Y. M. Lee, *Prog. Polym. Sci.* **2019**, *92*, 35.
[17] H. Ito, W. Oka, H. Goto, H. Umeda, *Jpn. J. Appl. Phys.* **2006**, *45*, 4325.
[18] J. Chen, C. T. Liu, *IEEE Access* **2013**, *1*, 150.
[19] Q. Zhang, C. Y. Tsai, L. J. Li, D. Liaw, *J. Nat. Commun.* **2019**, *10*, 1239.
[20] M. Hasegawa, D. Hirano, M. Fujii, M. Haga, E. Takezawa, S. Yamaguchi, A. Ishikawa, T. Kagayama, *J. Polym. Sci., Part A: Polym. Chem* **2013**, *51*, 575.
[21] M. Hasegawa, T. Ishigami, J. Ishii, K. Sugiura, M. Fujii, *Eur. Polym. J.* **2013**, *49*, 3657.
[22] M. Hasegawa, M. Horiuchi, K. Kumakura, J. Koyama, *Polym. Int.* **2013**, *63*, 486.
[23] G. Jiang, D. Wang, H. Du, X. Wu, Y. Zhang, Y. Tan, L. Wu, J. Liu, X. Zhang, *Polymer* **2020**, *12*, 413.
[24] G. Qian, H. Chen, G. Song, F. Dai, C. Chen, J. Yao, *Polymer* **2020**, *196*, 122482.
[25] M. Hasegawa, *Polymer* **2017**, *9*, 520.
[26] X. H. Yu, J. N. Liu, D. Y. Wu, *Mater. Today Commun.* **2019**, *21*, 100562.
[27] L. Bai, L. Zhai, M. He, C. Wang, S. Mo, L. Fan, *React. Funct. Polym.* **2019**, *141*, 155.
[28] L. Bai, L. Zhai, M. He, C. Wang, S. Mo, L. Fan, *Chin. J. Polym. Sci.* **2020**, *38*, 748.
[29] S. D. Kim, B. Lee, T. Byun, I. S. Chung, J. Park, I. Shin, N. Y. Ahn, M. Seo, Y. Lee, Y. Kim, W. Y. Kim, H. Kwon, H. Moon, S. Yoo, S. Y. Kim, *Sci. Adv.* **2018**, *4*, eaau1956.
[30] H. Lao, N. Mushtaq, G. Chen, H. Jiang, Y. Jiao, A. Zhang, X. Fang, *Polymer* **2020**, *206*, 122889.
[31] M. Hasegawa, Y. Watanabe, S. Tsukuda, J. Ishii, *Polym. Int.* **2016**, *65*, 1063.
[32] T. Matsumoto, E. Ishiguro, S. Komatsu, *J. Photopolym. Sci. Technol.* **2014**, *27*, 167.
[33] Y. Zhuang, R. Orita, E. Fujiwara, Y. Zhang, S. Ando, *Macromolecules* **2019**, *52*, 3813.
[34] S. Ando, T. Matsuura, S. Sasaki, *J. Polym. Sci., Part A: Polym. Chem* **1992**, *30*, 2285.
[35] A. I. Barzic, C. Hulubei, I. Stoica, R. M. Albu, *Macromol. Mater. Eng.* **2018**, *303*, 1800235.
[36] R. J. Tabar, C. T. Murray, R. S. Stein, *J. Polym. Sci. Part B: Polym. Phys.* **1983**, *21*, 831.
[37] G. Hou, Y. Liu, D. Zhang, G. Li, H. Xie, Z. Fang, *ACS Appl. Mater. Interfaces* **2020**, *12*, 31998.
[38] L. Qi, C. Y. Guo, M. G. Huangfu, Y. Zhang, L. M. Yin, L. Wu, J. G. Liu, X. M. Zhang, *Polymer* **2019**, *11*, 2055.
[39] D. McCoul, W. Hu, M. Gao, V. Mehta, Q. Pei, *Adv. Electron. Mater.* **2016**, *2*, 1500407.

How to cite this article: X.-X. Zhi, G.-L. Jiang, Y. Zhang, Y.-J. Jia, L. Wu, Y.-C. An, J.-G. Liu, Y. Liu, *J. Appl. Polym. Sci.* **2022**, *139*(4), e51544. https://doi.org/10.1002/app.51544